JBC Papers in Press. Published on July 23, 2019 as Manuscript RA119.008857
The latest version is at http://www.jbc.org/cgi/doi/10.1074/jbc.RA119.008857

The antibiotic robenidine exhibits guanabenz-like cytoprotective properties by a mechanism independent of protein phosphatase PP1:PPP1R15A

Zander Claes[1], Marloes Jonkhout[1], Ana Crespillo-Casado[2], Mathieu Bollen[1]

[1]Laboratory of Biosignaling & Therapeutics, KU Leuven Department of Cellular and Molecular Medicine, University of Leuven, B-3000 Leuven, Belgium;
[2]Cambridge Institute for Medical Research, University of Cambridge, Cambridge CB2 0XY, United Kingdom.

Running title: *Cytoprotective effects of robenidine*

Corresponding Author: Mathieu Bollen, KU Leuven, Campus Gasthuisberg, Herestraat 49, O&N1, PB901, B-3000 Leuven, Belgium. Phone: +32-16-33 06 44. E-mail: Mathieu.Bollen@kuleuven.be

Keywords: aminoguanidine, cell stress, eIF2α**,** guanabenz, protein misfolding, protein phosphatase 1, protein phosphatase 1 regulatory subunit 15A (PPP1R15A), robenidine, unfolded protein response (UPR)

ABSTRACT

The aminoguanidine compound robenidine is widely used as an antibiotic for the control of coccidiosis, a protozoal infection in poultry and rabbits. Interestingly, robenidine is structurally similar to guanabenz analogs, which currently undergo clinical trials as cytoprotective agents for the management of neurodegenerative diseases. Here, we show that robenidine and guanabenz to a similar degree protect cells from a tunicamycin-induced unfolded protein response (UPR). Both compounds also reduced the tumor necrosis factor alpha (TNFα)-induced activation of NFκB. The cytoprotective effects of guanabenz (analogs) have previously been explained by their ability to maintain eukaryotic translation initiation factor 2 subunit alpha (eIF2α) phosphorylation by allosterically inhibiting protein phosphatase PP1:PPP1R15A. However, using a novel split-luciferase based protein-protein interaction assay, we demonstrate here that neither robenidine nor guanabenz disrupt the interaction between PPP1R15A and either PP1 or eIF2α in intact cells. Moreover, both drugs also inhibited the UPR in cells that expressed a non-phosphorylatable mutant (Ser51Ala) of eIF2α. Our results identify robenidine as a PP1:PPP1R15A-independent cytoprotective compound that holds potential for the management of protein misfolding-associated diseases.

The unfolded-protein-response (UPR) is a cellular reaction to the accumulation of unfolded proteins in the endoplasmic reticulum (ER). This stress response aims to restore homeostasis in the ER by lowering protein translation rates, augmenting the number of folding chaperones, and increasing the degradation of misfolded proteins. This is achieved through different pathways originating from three different ER-stress sensors that are activated by unfolded proteins in the ER (1). One sensor is Inositol-responsive-enzyme-1 (IRE1), which catalyzes the splicing of the transcription factor XBP1 (X-box binding protein 1) mRNA, enabling the translation of functional XBP1 and the upregulation of target genes encoding ER chaperones and components of the ER-associated protein-degradation (ERAD) pathway (2). A second sensor is Activating-transcription-factor-6 (ATF6), which induces various stress-related genes following its translocation to the Golgi and subsequent proteolytic activation (3). The third sensor is protein-kinase-R-like-endoplasmic-reticulum-kinase (PERK), which phosphorylates the α subunit of eukaryotic translation initiation factor 2 (eIF2α) at Ser51 to reduce global translation whilst enhancing the translation of specific stress response genes such as *ATF4*, *CHOP*

and *PPP1R15A* (4). The latter branch of the UPR is also part of the more general integrated-stress-response (ISR) pathway. Importantly, the UPR and ISR are both regulated by a negative feedback loop that involves the delayed expression of PPP1R15A, also known as Growth-arrest-and-DNA-damage-induced-protein-34 (GADD34) or R15A, which forms a trimeric complex with protein phosphatase 1 (PP1) and G-actin (5,6). This PP1 holoenzyme counteracts UPR and ISR signaling through dephosphorylation of eIF2α at Ser51. The inhibition of eIF2α phosphatase(s) is generally considered to be an attractive therapeutic strategy for prolonging UPR signaling as it gives cells more time to cope with the detrimental effects of unfolded proteins, a hallmark of several neurodegenerative diseases (7,8).

Guanabenz is an aminoguanidine-type α_2-adrenoreceptor agonist developed during the 1980s as an anti-hypertensive drug but was later identified in a yeast-based screen as a compound with anti-prion activity (9). Subsequently, several groups demonstrated cytoprotective effects of guanabenz (analogs) in murine models of neurodegenerative diseases such as amyotropic lateral sclerosis (10), multiple sclerosis (11) and vanishing white-matter disease (12). The cytoprotective effects of guanabenz (analogs) have been explained by its ability to maintain eIF2α phosphorylation through inhibition of PP1:R15 (13). However, the molecular mechanism underlying the cytoprotective action of guanabenz (analogs) is controversial (14,15,16). Indeed, the proposed effects of guanabenz (analogs) on PP1:R15 complexes include such diverse mechanisms as disruption of the PP1:R15A interaction (10,13), interference with the recruitment of eIF2α (17), and targeting of R15B (a constitutively expressed R15 variant) for proteolytic degradation (18). Moreover, guanabenz (analogs) had no effect on the composition or activity of an *in vitro* reconstituted PP1:R15A:G-actin holoenzyme (16). Furthermore, guanabenz retained its cytoprotective effects in cells and organisms that lacked R15A or only expressed non-phosphorylatable eIF2α (Ser51Ala) (15). Despite the uncertainties concerning their mechanism of action, guanabenz (analogs) remain attractive therapeutics. Guanabenz itself has rapidly progressed to clinical trials using a drug-repurposing approach. A Phase I clinical trial to evaluate the pharmacokinetics of guanabenz in multiple sclerosis patients has been completed (NCT02423083), and a Phase II clinical trial for amyotrophic lateral sclerosis (EudraCT nr. 2014-005367-32) and early-childhood-onset vanishing white matter disease (EudraCT nr. 2017-001438-25) are ongoing.

Robenidine (1,2-bis[(E)-(4-chlorophenyl)methylideneamino]guanidine) is an aminoguanidine that has been used since the early 1970s to prevent coccidian infections in rabbits, chickens and turkeys (19,20). Often, animals are fed with robenidine-supplemented pellets (50 mg/kg food) during their entire life, except for a washout period before slaughter. The chronic and widespread use of robenidine as a food-supplement indicates that it is safe and well-tolerated, making it a suitable candidate-therapeutic for humans. Furthermore, robenidine belongs to the aminoguanidine compound class, which represents a diverse group of bioactive compounds used for the treatment of a broad range of diseases ranging from bacterial infections to cancer and diabetes, and many of these compounds are approved for human use (21). Despite its long history of use in animals, there have been no in-depth examinations of robenidine as a potential therapeutic for the treatment of human diseases. Here, we show that robenidine and guanabenz show similar cytoprotective effects in stressed cells. Furthermore, both compounds reduced the expression of UPR and ISR markers in stressed cells. Finally, using mutant cell lines and split-luciferase sensors, we demonstrate that the cytoprotective effects of robenidine do not involve changes in eIF2α phosphorylation or the eIF2α phosphatase PP1:R15A. Our data identify robenidine as a novel aminoguanidine with therapeutic potential for the treatment of protein-misfolding diseases.

RESULTS AND DICUSSION

Robenidine is a structural and functional analog of guanabenz

Using the PubChem search engine, we noticed structural similarities between robenidine and guanabenz (Fig. 1A). In contrast to guanabenz, robenidine has two substituted phenyl rings attached to its central aminoguanidine scaffold. In addition, these phenyl rings are *para*-chloro substituted while the phenyl ring of guanabenz has

two *ortho*-chloro substitutions. Further mining of the PubChem BioAssay database revealed that guanabenz and robenidine were both active in a high-throughput screen against the malaria-causing protozoan *Plasmodium Falciparum* (Fig. 1B) (22). Several anti-malarial drugs target the apicoplast (a non-photosynthetic plastid) through interference with its translational machinery (23). Interestingly, a similar mechanism of action was proposed for the cytoprotective properties of guanabenz in mammalian cells undergoing unfolded protein stress (24). These findings prompted us to explore whether robenidine has cytoprotective properties similar to those of guanabenz.

Cytoprotective effects of robenidine

The ER-stress induced UPR hampers cell-cycle progression and proliferation. Indeed, treatment of HeLa cells with tunicamycin, an inhibitor of protein glycosylation that induces the accumulation of misfolded proteins and activates the UPR, caused a dose-dependent decrease in proliferation, as derived from confluency assays with live-cell microscopy (Fig. 2A). This effect of tunicamycin can be rescued by guanabenz (13,17). Likewise, 5-20 μM robenidine reversed the proliferation defect of tunicamycin-treated HeLa cells in a dose-dependent manner (Fig. 2B). However, at higher concentrations of robenidine this cytoprotective effect was lost. We selected 15 μM of robenidine as an optimal concentration for treatment, as it produced nearly maximal cytoprotective effects but separated sufficiently from the higher, toxic concentrations. The cytoprotective effect of 15 μM robenidine was detected at relatively narrow tunicamycin concentrations of 400-800 ng/ml (Fig. 2C), similar to what has been reported for guanabenz (15). Guanabenz and robenidine were similarly cytoprotective at a concentration of 15 μM (Fig. 2D).

To evaluate whether drug-drug interactions exist between robenidine and guanabenz, we performed isobologram analysis (25). For this purpose, we first generated dose-response curves to accurately determine their EC50 values (Fig. 2E). These studies indicated that, on average, guanabenz is 10-15 times more potent than robenidine. Next, the isobologram was drawn by connecting the two axis intersection points (i.e., the EC50 for each drug alone), according to the 'Loewe Additivity' principle. Robenidine and guanabenz drug combinations were tested at 10:1 and 15:1 ratios and the corresponding EC50's of these combination regimens were plotted against the isobologram (Fig. 2F). The 95% confidence interval of the combination treatments overlapped with the 'Loewe Additivity' line, indicating that there are no synergistic or antagonistic interactions between robenidine and guanabenz.

Pyrimethamine shares structural features with robenidine as it also has a central guanidine scaffold and a *para*-chloro substituted phenyl ring (Fig. S1A). Moreover, pyrimethamine also displays potent anti-malarial activity (26). However, pyrimethamine was lethal at 10 μM (data not shown) and did not promote the survival of tunicamycin-treated HeLa cells at a sublethal dose of 3 μM (Fig. S1B).

Robenidine inhibits TNFα-induced NFκB activation

Guanabenz inhibits the TNFα-induced activation of the transcription factor NFκB (27). However, the concentration of guanabenz (200 μM) that was used in the latter study is toxic and far exceeds the concentrations that are routinely used to study its cytoprotective effects in cultured cells. Therefore, we tested whether robenidine and guanabenz affected NFκB activation at the more optimal concentration of 15 μM (Fig. 2). To this end, HEK293 cells were transfected with an NFκB-driven luciferase reporter plasmid and treated with TNFα concentrations of 0.1-10 ng/ml in the absence (CTRL) or presence of 15 μM robenidine (Fig. 3A). Robenidine significantly inhibited NFκB activation by TNFα concentrations between 0.1 and 0.3 ng/ml, with a maximal effect (inhibition of ~25%) at 0.3 ng/ml TNFα. A similar level of inhibition was observed with 15 μM guanabenz (Fig. 3B). We have ruled out that the observed reduction in bioluminescence was due to a loss of viable cells, as detected by MTT assays (Fig. S2).

Robenidine does not affect the interaction between R15A and PP1 or eIF2α

The cytoprotective effects of guanabenz (analogs) have been explained by an inhibitory effect on the eIF2α phosphatase PP1:R15A, resulting from a disruption of either the PP1:R15A interaction (13) or the recruitment of the substrate eIF2α (17). To examine whether guanabenz and robenidine

interfere with the binding of PP1 or eIF2α to R15A we designed NanoBiT split-luciferase sensors that report on PP1:R15A and eIF2α:R15A interactions in live cells (Fig. 4A). We fused the 19-kDa 'large-bit' (LgBiT) luciferase fragment to the N-terminus of PP1 and eIF2α. The 'small-bit' (SmBiT) luciferase fragment of 11 residues was inserted between the eIF2α-binding PEST-repeat region and the PP1-binding KVRF sequence of R15A. This insertion is unlikely to interfere with the activity or structure of R15A as the protein is almost completely unstructured in its native form. We envisaged that binding of LgBiT-PP1 or LgBiT-eIF2α to R15A-SmBiT would bring the split-luciferase fragments in close proximity, resulting in complementation and active luciferase (Fig. 4B). Indeed, transfection of HEK293T cells with LgBiT-PP1 + R15A-SmBiT or LgBiT-eIF2α + R15A-SmBiT resulted in luminescence, which was largely lost after deletion of the PEST region and mutation of the KVRF sequence to KARA (Fig. 4C and 4D). Co-immunoprecipitation analysis confirmed that FLAG-tagged R15A immunoprecipitated endogenous eIF2α and PP1, but this interaction was lost after deletion of the PEST region in combination with a mutation of the PP1-binding site (Fig. 4E). Together, these results indicated that the adopted split-luciferase sensors allowed the monitoring of the interaction of R15A with eIF2α and PP1 in live cells. We subsequently used these split-luciferase sensors to test whether guanabenz or robenidine affect the binding of LgBiT-eIF2α or LgBiT-PP1 to R15A-SmBiT in live cells. HEK293 cells transfected with the sensors were treated with 15 μM guanabenz or robenidine for 24 hours. However, we observed no reduction in luminescence signal (Fig. 4F). Furthermore, HEK293 cells transfected with a constitutively active split-luciferase showed no effect of the compounds on cell viability or luciferase activity. Together these results indicated that cytoprotective concentrations of guanabenz and robenidine do not measurably affect PP1:R15A or eIF2α:R15A interactions, as measured with transient, CMV-driven expression of split-luciferase sensors in live cells.

Robenidine inhibits the UPR and ISR

The cytoprotective effects of guanabenz in conditions of ER stress have been attributed to its inhibitory effect on the UPR and the ISR (10). To investigate whether robenidine acts through the same mechanism, we used CHO cells containing reporters for both the ISR (CHOP::GFP) and the UPR branch that involves IRE1 (XBP1s::Turquoise) (15). Flow cytometry analysis disclosed a clear induction of both genes following the addition of 175 ng/ml tunicamycin for 55 hours (Fig. 5A). Co-treatment of these cells with 15 μM of either robenidine or guanabenz decreased the expression of CHOP and XBP1s by 40-60% (Fig. 5B).

A previous study showed that guanabenz (analogs) retain their cytoprotective activity in cells that express a non-phosphorylatable eIF2α mutant (15). This finding contradicts the proposal that guanabenz's cytoprotective effects are mediated by an increased phosphorylation of eIF2α at Ser51(8,24). To examine whether the inhibition of the expression of CHOP and XBP1s by robenidine and guanabenz are mediated by an increased eIF2α phosphorylation we used a variant CHO reporter cell line that expresses non-phosphorylatable eIF2α (Ser51Ala). Consistent with ISR-dependent CHOP activation, the activation of the CHOP::GFP reporter was less pronounced in the cell line expressing eIF2α Ser51Ala (compare Figs. 5A and 5C). Nonetheless, both robenidine and guanabenz inhibited the induction of CHOP::GFP and XBP1s::Turquoise in the mutant cell line upon treatment with tunicamycin (Fig. 5D). These results demonstrate that robenidine, like guanabenz, does not exert its cytoprotective effect by increasing the phosphorylation of eIF2α at Ser51.

CONCLUSIONS

Here, we have identified robenidine as a new aminoguanidine compound with cytoprotective properties, similar to those previously described for the analogues salubrinal (28), guanabenz (13), sephin1 (10) and raphin1 (18). Indeed, robenidine reduced the anti-proliferative effects of tunicamycin (Fig. 2), dampened TNFα-induced NFκB activation (Fig. 3), and inhibited the expression of ISR and UPR markers (Fig. 5). We also found that the cytoprotective effects of robenidine and guanabenz could not be explained by disruption of R15A:PP1 or R15A:eIF2α, and were not mediated by changes in the phosphorylation state of eIF2α (Fig. 5). These

results therefore demonstrate that the phenotypic effects of these drugs cannot be mediated by an inhibition of the R15A-PP1-actin holoenzyme or an altered phosphorylation of eIF2α at Ser51. Similar conclusions were recently drawn for guanabenz and sephin1 (15,28), but are at variance with reports hinting at inhibitory effects of guanabenz (analogs) on PP1:R15 assembly and its recruitment of eIF2α as a substrate (10,17).

Other targets of guanabenz (analogs) that have been proposed to underly their cytoprotective function are cholesterol 25-hydroxylase (29), ribosomal RNA (30) and lipid membranes (31). It is currently uncertain whether the antibacterial, anti-inflammatory and cytoprotective properties of robenidine and guanabenz (analogs) arise from the same cellular target(s), but this seems likely as both compounds had very similar effects at high nanomolar to low micromolar concentrations. The identification of the cellular target(s) of robenidine and guanabenz (analogs) remains an important goal for further exploration, as it will aid the development of analogs with higher potency.

We show here for the first time that guanabenz and robenidine significantly inhibit the activation of NFκB (Fig. 3). However, this effect was rather small (~25% inhibition) and therefore unlikely to contribute significantly to the cytoprotective properties of these compounds. At present, we cannot exclude that the inhibitory effects of robenidine and guanabenz in the NFκB and CHOP/XBP1s reporter cell lines (Fig. 3 and Fig. 5) are (partially) explained by a general inhibitory effect on protein translation, as the assays rely on the production of luciferase and fluorescent protein for signal readout.

Guanabenz, sephin1 and raphin1 have shown promising results in various murine models of neurodegenerative diseases (10,11,18). We speculate that robenidine has a similar therapeutic potential, in particular since its widespread industrial use for nearly 50 years as a food-additive and coccidostat documents its safety and tolerance, at least in animals. Pharmacokinetic studies in rabbits showed that robenidine is orally available and has a moderate half-life of around 12 hours (32). Micromolar serum concentrations are reached with a single oral dose, which are the concentrations needed for cytoprotective effects *in vitro* (Fig. 2). Our isobolographic analysis suggests that there is no benefit of combining robenidine and guanabenz (analogs). Nonetheless, our studies indicate that robenidine is an attractive candidate for preclinical testing in animal models of neurodegenerative diseases.

EXPERIMENTAL PROCEDURES

Materials

The following antibodies were used: FLAG (Sigma-Aldrich, F1804), Beta Actin (GeneTex, GTX26276), PP1 (made in-house, (33)), eIF2α (ThermoFisher Scientific, AHO0802) and secondary HRP-tagged antibodies were purchased from Agilent-Dako. Guanabenz was purchased from TCI Europe (G0456), robenidine from Acros Organics NV (459400010), tunicamycin from SanBio BV (11445), human TNFα from Sigma-Aldrich (SRP3177), Coelenterazine from Carl Roth GMBH (4094.3), D-luciferin from SanBio BV (14682-50) and Pyrimethamine from Acros Organics NV (461200010). Split-luciferase sensors were made using ligation-independent cloning techniques. LgBiT was fused via a 15 amino acid flexible linker (GSSGGGGSGGGGSSG) to the N-terminus of full length PP1α or eIF2α. SmBiT was inserted at residue 537 of R15A with a 5-residue flexible linker (GSTSG) at both ends. A constitutively active NanoBiT luciferase that served as a control consisted of LgBiT fused to SmBiT via a 15 amino acid flexible linker.

PubChem database searching

The guanabenz entry was accessed (https://pubchem.ncbi.nlm.nih.gov/) under PubChem CID 5702063. Robenidine (CID 9570438) was identified through the 'related record' search function, focusing on substituted aminoguanidines. High-throughput assays that tested both compounds were identified manually under the 'BioAssay results' section. Subsequently, the BioAssay AIDs (assay identification numbers) were used to query the obtained potency for each compound. MarvinSketch was used for drawing and exporting chemical structures (MarvinSketch, 17.21.0, ChemAxon).

Cytoprotection experiments

HeLa cells were plated at approximately 10% confluency in transparent 96-well plates. Three technical replicates were used per condition.

Treatment with compounds started at the time of seeding. All compounds were dissolved in DMSO. The final concentration of DMSO was the same in all conditions of each experiment and never exceeded 0.5%. Proliferation was measured using an IncuCyte ZOOM system and analyzed using IncuCyte ZOOM software (Essen BioScience).

Isobologram analysis

Cytoprotection experiments were performed as described above. The EC50 isobole was generated by performing three dose-response experiments, for both robenidine and guanabenz. From these data, the average EC50 for both drugs was calculated and used as intercepts of the isobologram. Next, dose-response experiments were performed for the indicated robenidine-guanabenz combination ratios and the calculated EC50's were plotted individually on the isobolograph. Calculation of EC50's was performed using the four-parameter model with variable slope with GraphPad Prism V5.

NFκB reporter assay

HEK293 cells were transfected with an NF-κB driven firefly luciferase-reporter plasmid (Addgene 14886) for 24 hours. Subsequently, the cells were seeded in white opaque 96-well plates at approximately 50% confluency and treated with the indicated concentrations of TNFα, guanabenz and/or robenidine. A minimum of four technical replicates were used per condition. The final concentration of DMSO was identical in all experimental conditions and never exceeded 0.5%. One day after seeding and treatment of the cells, firefly activity was measured on a Luminoskan Ascent (Thermo Scientific, USA), after replacement of the cell culture medium with homemade firefly assay buffer (0.5% Triton-X100, 50 mM Tris at pH 7.4, 5 mM MgCl2, 20 µM pyrophosphate, 500 µM ATP and 150 µg/ml D-luciferin). As firefly luciferase exhibits flash-type kinetics, the signal was measured in the stable phase, which typically occurred 3-4 minutes after incubation with firefly assay buffer. To account for possible variations in cell proliferation between the different conditions, a parallel plate of HEK293 cells was seeded and treated identically to the firefly assay plate. At the time of luciferase measurement, cell proliferation was measured in the parallel plate using MTT assays. For this, 3-(4,5-dimethylthiazol-2-yl)-2,5-diphenyltetrazolium bromide dissolved in TRIS buffer at pH 7.4 was added at a final concentration of 0.5 mg/ml to the assay medium and incubated overnight. Formazan crystals were dissolved in DMSO, transferred to a transparent 96-well plate and the absorbance was measured at 550 nm using a BioTek ELx808 microplate reader.

Flow cytometry with CHO reporter cell lines

CHO cells were plated in 6-well plates at approximately 20% confluency and treated with the indicated concentration of compounds for 55 hours. Three technical replicates were included per condition. The final concentration of DMSO (< 0.5%) was the same in all conditions. Cell culture medium and compounds were refreshed halfway through the incubation period to prevent medium evaporation and stressing the cells. Subsequently, cells were washed, harvested in PBS and used for flow cytometry. GFP and Turquoise expression were measured on a BD FACSCanto II HTS system using the following filters: GFP: Ex. 488 nm, Em. 500-560 nm; Turquoise: Ex. 405 nm, Em. 400-500 nm**.** At least 10,000 cells were recorded per sample. Dead cells were excluded based on the scatter profile of a calibration sample containing 50% dead and 50% live cells. Data was processed using FlowJo software (Tree Star, Inc.).

NanoBiT split-luciferase assay

HEK293 cells were plated at approximately 20% confluency and transfected with indicated split-luciferase sensors for 48 hours. To achieve sufficient sensor activity, sensors were cloned in vectors containing the CMV promoter and not in the weaker TK promoter-driven vectors of the NanoBiT kit. Subsequently, the cells were harvested and resuspended in PBS. The luciferase substrate coelenterazine was added to the cell suspension at a final concentration of 25 µM and cells were dispensed at approximately 10,000 cells/well in white 96-well plates. Luciferase activity was measured on a Luminoskan Ascent (Thermo Scientific, USA). When the cells were treated with compounds, they were reseeded in opaque 96-well plates after the 48 hour transfection period. A minimum of three technical replicates were used per condition. To correct for effects of the compounds on cell proliferation or expression of the split-luciferase sensors, a third batch of cells, expressing a constitutively active NanoBiT

luciferase (see 'Materials' section), was seeded and treated in parallel.

Cell culture

HEK293 cells (ATCC, Molsheim, France) were cultured in Dulbecco's modified Eagle's medium with high glucose (4,500 mg/L glucose; Sigma-Aldrich), containing 10% fetal calf serum (Sigma-Aldrich), 100 U/ml penicillin and 100 µg/ml Streptomycin. HeLa cells (ATCC, Molsheim, France) were cultured in the same medium but with 1,000 mg/L glucose. Transfections were performed with jetPRIME (Polyplus, New York, USA). All cell lines were mycoplasma free.

Biochemical techniques

HEK293 cells were lysed with lysis buffer (50 mM Tris-HCl at pH 7.4, 0.01 % saponine, 150 mM NaCl, 10% glycerol), supplemented with protease inhibitors (0.5 mM phenylmethanesulfonyl fluoride, 0.5 mM benzamidine, 5 µM leupeptin). Subsequently, lysates were sonicated with three 10-second cycles at high intensity and cleared by centrifugation at 10,000 x g. For FLAG traps, cleared cell lysates were incubated with 20 µL FLAG affinity beads (Sigma, cat. no. P4333) for 2-3h at 4°C. Beads were then washed once with PBS and subjected to Immunoblotting. SDS-PAGE gel electrophoresis was performed with 10% or 4-12% Bis-Tris (NuPAGE, Invitrogen). Immunoblots were visualized using ECL reagent (Perkin Elmer) in an ImageQuant LAS4000 imaging system (GE Healthcare). The signals were quantified using Image J (USA NIH).

Acknowlegdements

We thank David Ron (University of Cambridge) for feedback on the manuscript and for the generous gift of UPR and ISR reporter cell lines. Flow cytometry/FACS was performed at the VIB-KU Leuven FACS Core Facility. We thank Martial Luyts (L-BioStat, University of Leuven) for advice regarding statistics.

Conflict of interest

The authors declare no conflict of interests**.**

Author Contributions

ZC designed and performed all experiments, and analysed the data. MJ contributed to the execution of the flow cytometry experiments. ACC generated the UPR and ISR reporter cell lines and gave feedback on the manuscript. ZC and MB wrote the manuscript. MB coordinated the project.

REFERENCES

1. Walter, P., and Ron, D. (2011) The unfolded protein response: from stress pathway to homeostatic regulation. *Science*. **334**, 1081-6
2. Mori, K. (2000) Tripartite Management of Unfolded Proteins in the Endoplasmic Reticulum. *Cell*. **101**, 451-4
3. Shen, J., Chen, X., Hendershot, L., and Prywes, R. (2002) ER Stress Regulation of ATF6 Localization by Dissociation of BiP / GRP78 Binding and Unmasking of Golgi Localization Signals. *Dev Cell*, **3**, 99–111
4. Cao, S. S., and Kaufman, R. J. (2012) Unfolded protein response. *Current Biology*. **22**, R622–R626
5. Chambers, J. E., Dalton, L. E., Clarke, H. J., Malzer, E., Dominicus, C. S., Patel, V., Moorhead, G., Ron, D., and Marciniak, S. J. (2015) Actin dynamics tune the integrated stress response by regulating eukaryotic initiation factor 2 α dephosphorylation. *Elife*. 10.7554/eLife.04872
6. Yan, Y., Crespillo-casado, A., Clarke, H. J., Harding, H. P., Marciniak, S. J., Read, R. J., and Ron, D. (2015) G-actin provides substrate-specificity to eukaryotic initiation factor 2 α holophosphatases. *Elife*. 10.7554/eLife.04871

7. Sundaram, J. R., Lee, I. C. J., and Shenolikar, S. (2017) Translating protein phosphatase research into treatments for neurodegenerative diseases. *Biochem Soc Trans*. **45**, 101-112
8. Schneider, K., and Bertolotti, A. (2015) Surviving protein quality control catastrophes - from cells to organisms. *J. Cell Sci*. **128**, 3861–3869
9. Tribouillard-Tanvier, D., Béringue, V., Desban, N., Gug, F., Bach, S., Voisset, C., Galons, H., Laude, H., Vilette, D., and Blondel, M. (2008) Antihypertensive drug guanabenz is active in vivo against both yeast and mammalian prions. *PLoS One*. 10.1371/journal.pone.0001981
10. Das, I., Krzyzosiak, A., Schneider, K., Wrabetz, L., Antonio, M. D., Barry, N., Sigurdardottir, A., and Bertolotti, A. Preventing proteostasis diseases by selective inhibition of a phosphatase regulatory subunit. *Science*. **348**, 239-242
11. Way, S. W., Podojil, J. R., Clayton, B. L., Zaremba, A., Collins, T. L., Kunjamma, R. B., Robinson, A. P., Brugarolas, P., Miller, R. H., Miller, S. D., and Popko, B. (2015) Pharmaceutical integrated stress response enhancement protects oligodendrocytes and provides a potential multiple sclerosis therapeutic. *Nat. Commun*. **6**, 1–13
12. Dooves, S., Bugiani, M., Wisse, L. E., Abbink, T. E. M., and Knaap, M. S. Van Der (2017) Bergmann glia translocation : a new disease marker for vanishing white matter identifies therapeutic effects of Guanabenz treatment. *Neuropathol Appl Neurobiol*. **44**, 391-403
13. Tsaytler, P., Harding, H. P., Ron, D., and Bertolotti, A. (2011) Selective inhibition of a regulatory subunit of protein phosphatase 1 restores proteostasis. *Science*. **332**, 91–4
14. Peti, W., Nairn, A. C., and Page, R. (2013) Structural basis for protein phosphatase 1 regulation and specificity. *FEBS J*. **280**, 596–611
15. Crespillo-Casado, A., Chambers, J. E., Fischer, P. M., Marciniak, S. J., and Ron, D. (2017) PPP1R15A-mediated dephosphorylation of eIF2α is unaffected by Sephin1 or Guanabenz. *Elife*. 10.7554/eLife.26109
16. Crespillo-Casado A., Claes Z., Choy MS., Wolfgang P., Bollen M., R. D. (2018) A Sephin1insensitive tripartite holophosphatase dephosphorylates translation initiation factor 2alpha. *J Biol Chem*. **293**, 7766–7776
17. Carrara, M., Sigurdardottir, A., and Bertolotti, A. (2017) Decoding the selectivity of eIF2α holophosphatases and PPP1R15A inhibitors. *Nat Struct & Mol Biol*. **24**, 708-716
18. Krzyzosiak, A., Sigurdardottir, A., Luh, L., Carrara, M., Das, I., Schneider, K., Bertolotti, A.(2018) Target-Based Discovery of an Inhibitor of theRegulatory Phosphatase PPP1R15B. *Cell*. **174**, 1216-1228
19. Kantor S., Kennett LR., W. E. (1970) 1,3-Bis(p-chlorobenzylideneamino)guanidine Hydrochloride (Robenzidene): New Poultry Anticoccidial Agent. *Science*. **168**, 373-4
20. European Food Safety Authority (2011) Scientific Opinion on safety and efficacy of Cycostat ® 66G (robenidine hydrochloride) for rabbits for breeding and fattening. *EFSA J*. 10.2903/j.efsa.2011.2102
21. Sączewski, F., and Balewski, Ł. (2013) Biological activities of guanidine compounds, 2008 – 2012 update. *Expert Opin. Ther. Pat*. **23**, 965–995
22. National Center for Biotechnology Information. PubChem BioAssay Database; AID=504834, https://pubchem.ncbi.nlm.nih.gov/bioassay/504834 (accessed July 28, 2018)
23. Botté, C. Y., Dubar, F., McFadden, G. I., Maréchal, E., and Biot, C. (2012) Plasmodium falciparum apicoplast drugs: Targets or off-targets? *Chem. Rev*. **112**, 1269–1283
24. Tsaytler, P., and Bertolotti, A. (2013) Exploiting the selectivity of protein phosphatase 1 for pharmacological intervention. *FEBS J*. **280**, 766–770
25. Foucquier, J., and Guedj, M. (2015) Analysis of drug combinations: current methodological

landscape. *Pharmacol. Res. Perspect.* **3(3)**:e00149

26. McCollum, A. M., Poe, A. C., Hamel, M., Huber, C., Zhou, Z., Shi, Y. P., Ouma, P., Vulule, J., Bloland, P., Slutsker, L., Barnwell, J. W., Udhayakumar, V., and Escalante, A. a (2006) Antifolate resistance in Plasmodium falciparum: multiple origins and identification of novel dhfr alleles. *J. Infect. Dis.* **194**, 189–197
27. Nakajima, S., Chi, Y., Gao, K., Kono, K., and Yao, J. (2015) eIF2 α -Independent Inhibition of TNF- α -Triggered NF- κ B Activation by Salubrinal. *Biol Pharm Bull.* **38**, 1368–1374
28. Boyce, M., Bryant, K. F., Jousse, C., Long, K., Harding, H. P., Scheuner, D., Kaufman, R. J., Ma, D., Coen, D. M., Ron, D., and Yuan, J. (2005) A selective inhibitor of eIF2alpha dephosphorylation protects cells from ER stress. *Science.* **307**, 935–939
29. Perego, J., Mendes, A., Bourbon, C., Camosseto, V., Combes, A., Liu, H., Manh, T. V., Dalet, A., Chasson, L., Spinelli, L., Bardin, N., Chiche, L., Santos, M. A. S., Gatti, E., and Pierre, P. (2018) Guanabenz inhibits TLR9 signaling through a pathway that is independent of eIF2a dephosphorylation by the GADD34 / PP1c complex. *Sci Signal*. 10.1126/scisignal.aam8104
30. Nguyen, P. H., Hammoud, H., Halliez, S., Pang, Y., Evrard, J., Schmitt, M., Oumata, N., Bourguignon, J. J., Sanyal, S., Beringue, V., Blondel, M., Bihel, F., and Voisset, C. (2014) Structure-activity relationship study around guanabenz identifies two derivatives retaining antiprion activity but having lost α2-adrenergic receptor agonistic activity. *ACS Chem. Neurosci.* **5**, 1075–1082
31. Ogunniyi, A. D., Khazandi, M., Stevens, A. J., Sims, S. K., Page, S. W., Garg, S., Venter, H., Powell, A., White, K., Petrovski, K. R., Laven-Law, G., Tótoli, E. G., Salgado, H. R., Pi, H., Coombs, G. W., Shinabarger, D. L., Turnidge, J. D., Paton, J. C., McCluskey, A., and Trott, D. J. (2017) Evaluation of robenidine analog NCL195 as a novel broad-spectrum antibacterial agent. *PLoS One*. 10.1371/journal.pone.0183457
32. Jacques E. Tulliez, Elizabeth F. Durand, and G. F. B. (1982) Metabolic fate and pharmacokinetics of tissue residues of the anticoccidial drug robenidine in the rabbit. Incidence of coprophagy on its bioavailability. J. *Agric. Food Chem*, **30**, 1071-1075
33. Van Dessel, N., Beke, L., Görnemann, J., Minnebo, N., Beullens, M., Tanuma, N., Shima, H., Van Eynde, A., and Bollen, M. (2010) The phosphatase interactor NIPP1 regulates the occupancy of the histone methyltransferase EZH2 at Polycomb targets. *Nucleic Acids Res.* **38**, 7500–7512

FOOTNOTES

This work was supported by the Bijzonder Onderzoeksfonds (BOF-GOA 15/016]. Zander Claes is supported by a PhD grant of the Research Foundation Flanders (FWO).

Abbreviations

ATF6, activating transcription factor 6; CHOP, C/EBP homologous protein; eIF2α, Eukaryotic Initiation Factor 2 alpha; ER, endoplasmic reticulum; ERAD, ER-associated protein degradation; IRE1, Inositol-responsive enzyme 1; ISR, integrated stress response; NFκB, nuclear factor kappa-light-chain-enhancer of activated B cells; PERK, protein kinase R like endoplasmic reticulum kinase; PP1, protein phosphatase 1; TNFα, Tumor necrosis factor alpha; UPR, unfolded protein response; XBP1, X-box binding protein 1

LEGENDS TO THE FIGURES

Fig. 1. Structural and bioactive similarities between robenidine and guanabenz. (A) Chemical structure of guanabenz and robenidine. **(B)** Table showing the inhibitory potency (50% effective concentration, EC_{50}) of guanabenz and robenidine in a quantitative high-throughput screen against *Plasmodium Falciparium* apicoplast development. The data were extracted from the PubChem database using the indicated BioAssay AIDs (Assay Identification number)

Fig. 2. Robenidine protects HeLa cells from tunicamycin-induced toxicity. (A) Proliferation of HeLa cells treated with the indicated concentrations of tunicamycin for 3 days. **(B)** Dose-dependent rescue of HeLa cells treated with 400 ng/ml tunicamycin (3 days) by the indicated concentrations of robenidine. The data were analyzed with one-way ANOVA using Dunnet's post hoc test. **(C)** Proliferation of HeLa cells treated for 4 days with or without 15 µM robenidine at the indicated concentrations of tunicamycin. Two-way ANOVA analysis indicated that both tunicamycin ($F_{5,24}$=197.1, p<0.001) and robenidine ($F_{1,24}$=130.7, p<0.001) significantly affected the proliferation of the cells. Additionally, there was an interaction of the two factors regarding their effects on proliferation ($F_{5,24}$=13, p<0.001). Tukey's post hoc test was finally used to compare control versus robenidine for every concentration of tunicamycin. **(D)** Comparison of the cytoprotective effect of 15 µM guanabenz or robenidine in Hela cells treated with tunicamycin for 3 days. The data were analyzed with one-way ANOVA using Tukey's post hoc test. **(E)** Dose-response relationship of the cytoprotective effect of robenidine or guanabenz on HeLa cells treated with 400 ng/ml tunicamycin for 3 days. Curves were fitted using a four-parameter model with variable slope. For each concentration, the average of three technical repeats is presented. **(F)** Isobologram analysis of robenidine (R) and guanabenz (G) combination treatments at the indicated dose ratios. EC50's of dose-response experiments are plotted. Black open and closed dots represent the mean with 95% confidence intervals of 15:1 and 10:1 combination treatments respectively. The 'Loewe Additivity' line (black line) represents all theoretical robenidine-guanabenz combinations resulting in 50% cytoprotective effect, assuming both drugs interact in an additive manner. Datapoints to the left of the curve are synergistic combinations, while datapoints to the right are antagonistic. All panels except panel F show one of at least three independent experiments. Panels A-D show individual datapoints of at least three technical replicates with bar graphs indicating the mean and error bars the standard deviation (n.s., not significant, = p>0.05; *p<0.05; **p<0.01; ***p<0.001).

Fig. 3. Robenidine inhibits NFκB activation by TNFα. (A) HEK293 cells were transfected with a NFκB-driven luciferase reporter plasmid. After 24 hours the cells were treated for an additional 24 hours with vehicle (CTRL) or 15 µM robenidine, and the indicated concentrations of TNFα. NFκB activity was derived from firefly bioluminescence assays and was plotted as a percentage of the activity in cells treated with TNFα alone (CTRL). Two-way ANOVA analysis indicated that both TNFα ($F_{5,231}$=2.6, p=0.024) and robenidine ($F_{1,231}$=130.7, p<0.001) significantly affected the activation of NFκB. Additionally, there was an interaction of the two factors regarding their effects on NFκB activation ($F_{5,231}$=3.3, p=0.0065). Tukey's post hoc test was finally used to compare control versus robenidine for every concentration of TNFα. **(B)** Same as in (A) but cells were treated with 0.3 ng/ml TNFα with or without the indicated concentrations of robenidine and/or guanabenz. Statistical analysis was performed using one-way ANOVA with Tukey's post hoc test. Datapoints show all technical replicates from three independent experiments, with the means represented by bar graphs and error bars indicating the standard deviation (n.s., not significant, = p>0.05; *p<0.05; ***p<0.001).

Fig. 4. **Robenidine does not affect the interaction between R15A and PP1 or eIF2α. (A)** Cartoon representation of the fusions used for the split-luciferase sensors. R15A is shown in beige, PP1 in red and eIF2α in green. The eIF2α-recruiting PEST domain is shown as grey repeats and the position of the SmBiT or LgBiT split-luciferase tags are shown in cyan. FLAG-tag and the PP1-binding KVRF sequence (or the corresponding PP1-binding mutant, KARA) are indicated. **(B)** Cartoon showing the principle of the split-

luciferase sensors: binding of wild-type R15A-SmBiT to either LgBiT-eIF2α or LgBiT-PP1 produces an active luciferase through complementation of SmBiT and LgBiT. **(C)** Bioluminescent signal of live HEK293 cells transfected with combinations of split-luciferase sensors, as shown in panel A. All technical replicates of 3 independent experiments were plotted as a percentage of wild-type R15:PP1 or R15A:eIF2α sensor signal. Bar graphs indicate the mean and error bars the standard deviation. **(D)** Immunoblot of HEK293 lysates from the experiment shown in panel C. **(E)** HEK293 cells were transfected with SmBit-tagged wild type (WT) or mutant (M) R15A variants, as shown in panel A. FLAG traps of cell lysates were analyzed by immunoblotting. The data shown is representative for three independent experiments. **(F)** Bioluminescent signal of live HEK293 cells transfected for 48 hours with the indicated constructs and treated with guanabenz or robenidine for 24 hours. A constitutively active luciferase construct served as a control for interference of the compounds with cell viability or luciferase activity. All technical replicates of three independent experiments were plotted as a percentage of the untreated control with bar graphs indicating the mean and error bars the standard deviation. For all experiments, statistical analysis was performed using one-way ANOVA with Tukey's post hoc test (n.s., not significant, = $p>0.05$; ***$p<0.001$).

Fig. 5. Robenidine inhibits the UPR and ISR independent of eIF2α phosphorylation. (A) Representative graph of the two-dimensional plot of the fluorescence signals from wild-type CHO reporter cells stably transduced with both a CHOP::GFP reporter (reflecting ISR activity) and a XBP1::Turquoise reporter (reflecting IRE1α activity), treated with or without tunicamycin and/or robenidine, and analyzed with flow cytometry. Histograms of the distribution of the two reporter signals in the three treatment conditions are plotted on the corresponding axes. **(B)** Scatterplots of the median fluorescence signals of wild-type CHO reporter cells treated for 55 hours with the indicated concentrations of tunicamycin, robenidine and guanabenz, and analyzed by flow cytometry. Bar graphs indicate the mean and error bars the standard deviation. **(C)** As in panel 4A, but with CHO reporter cells expressing eIF2α-Ser51Ala. **(D)** As in panel 4B, but with CHO reporter cells expressing eIF2α-Ser51Ala. For panels B and D, all technical replicates from 4 independent experiments were plotted. Statistical analysis was performed using one-way ANOVA with Dunnet's post hoc test (**$p<0.01$; ***$p<0.001$).

Figure 1

A

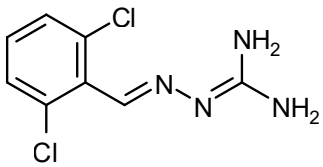

Guanabenz

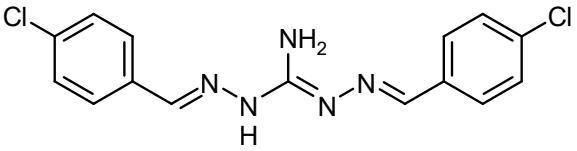

Robenidine

B

BioAssay name (AID)	Compound	Activity (EC_{50}, µM)
Primary qHTS for delayed death inhibitors of the malarial parasite plastid, 48 hour incubation (504832)	Guanabenz	13.46
	Robenidine	0.76
Primary qHTS for delayed death inhibitors of the malarial parasite plastid, 96 hour incubation (504834)	Guanabenz	3.70
	Robenidine	0.85

Figure 2

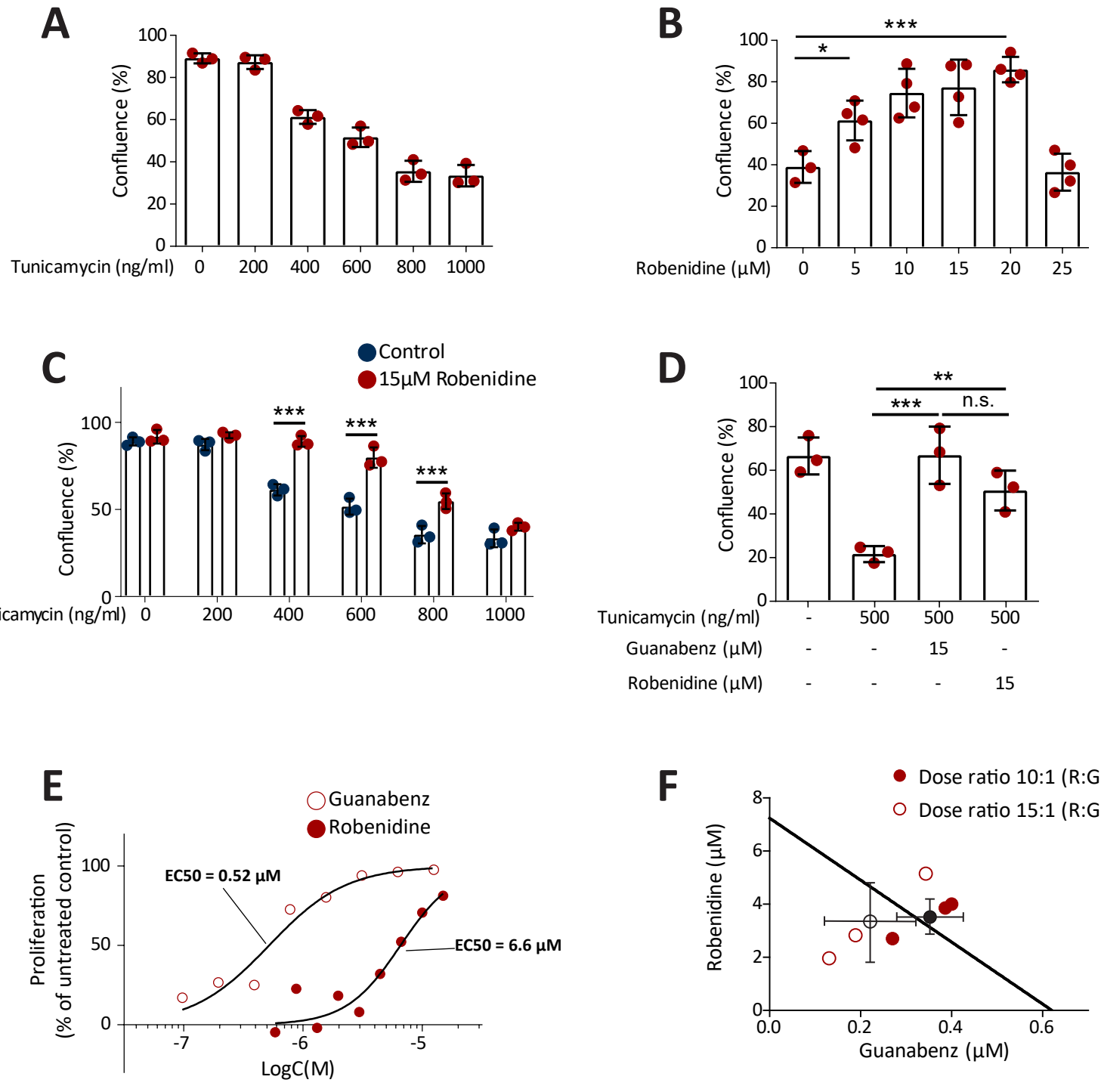
A
Confluence (%)
Tunicamycin (ng/ml)
B
Confluence (%)
Robenidine (µM)
C
Control
15µM Robenidine
Confluence (%)
Tunicamycin (ng/ml)
D
Confluence (%)
Tunicamycin (ng/ml)
Guanabenz (µM)
Robenidine (µM)
n.s.
E
Guanabenz
Robenidine
EC50 = 0.52 µM
EC50 = 6.6 µM
Proliferation
(% of untreated control)
LogC(M)
F
Dose ratio 10:1 (R:G)
Dose ratio 15:1 (R:G)
Robenidine (µM)
Guanabenz (µM)

Figure 3

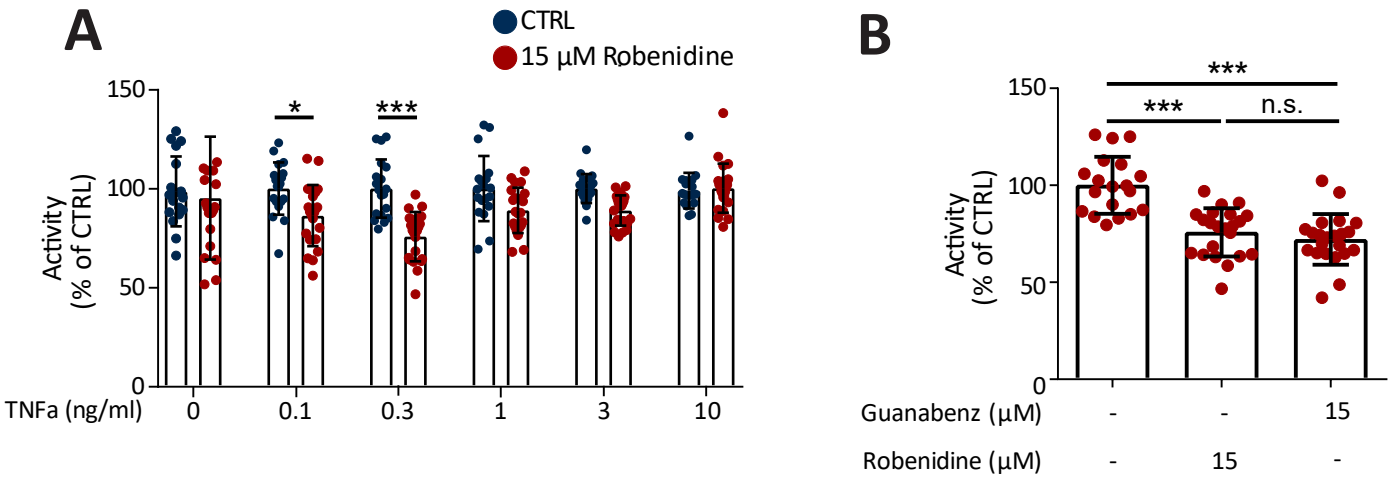
A
CTRL
15 µM Robenidine
Activity (% of CTRL)
150
100
50
0
*
***
TNFa (ng/ml)
0
0.1
0.3
1
3
10
B
***
***
n.s.
Activity (% of CTRL)
150
100
50
0
Guanabenz (µM)
-
-
15
Robenidine (µM)
-
15
-

Figure 4

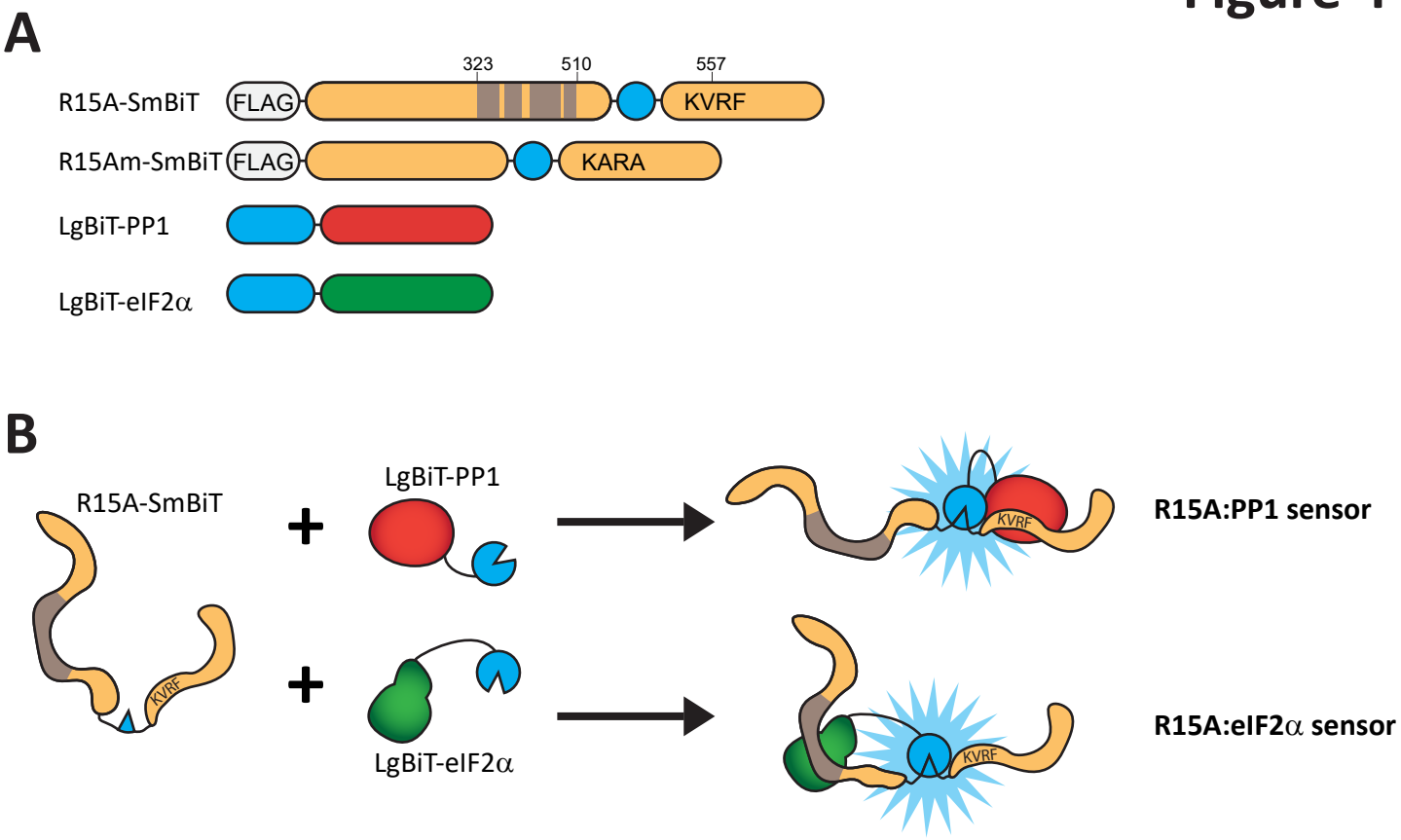
A
323
510
557
R15A-SmBiT
FLAG
KVRF
R15Am-SmBiT
FLAG
KARA
LgBiT-PP1
LgBiT-eIF2α
B
R15A-SmBiT
LgBiT-PP1
KVRF
R15A:PP1 sensor
LgBiT-eIF2α
KVRF
R15A:eIF2α sensor

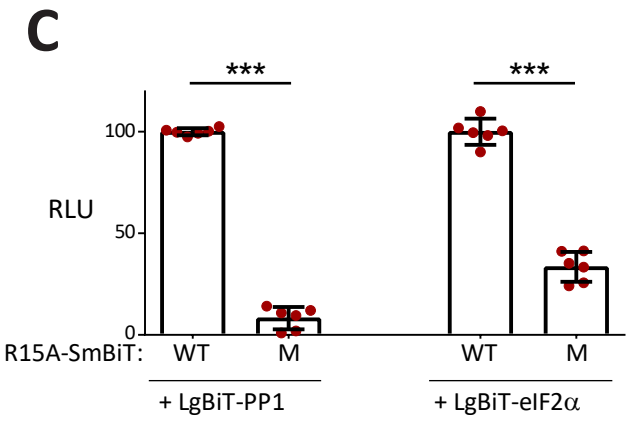
C
***
***
RLU
100
50
0
R15A-SmBiT: WT M WT M
+ LgBiT-PP1
+ LgBiT-eIF2α

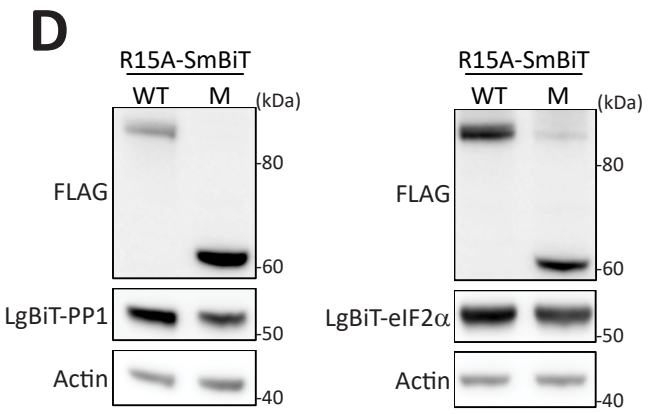
D
R15A-SmBiT
WT M (kDa)
FLAG
80
60
LgBiT-PP1
50
Actin
40
R15A-SmBiT
WT M (kDa)
FLAG
80
60
LgBiT-eIF2α
50
Actin
40

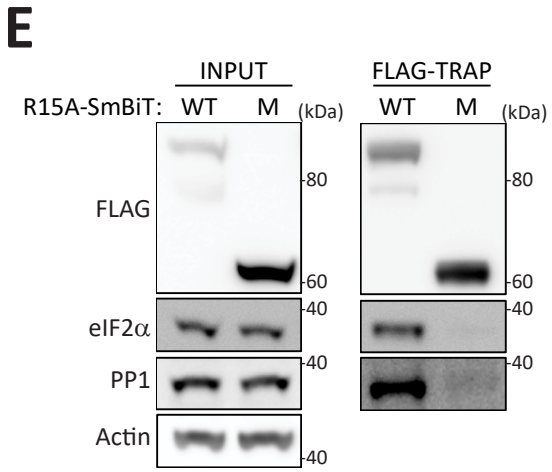
E
INPUT
FLAG-TRAP
R15A-SmBiT: WT M (kDa)
WT M (kDa)
FLAG
80
60
eIF2α
40
PP1
40
Actin
40
80
60
40
40

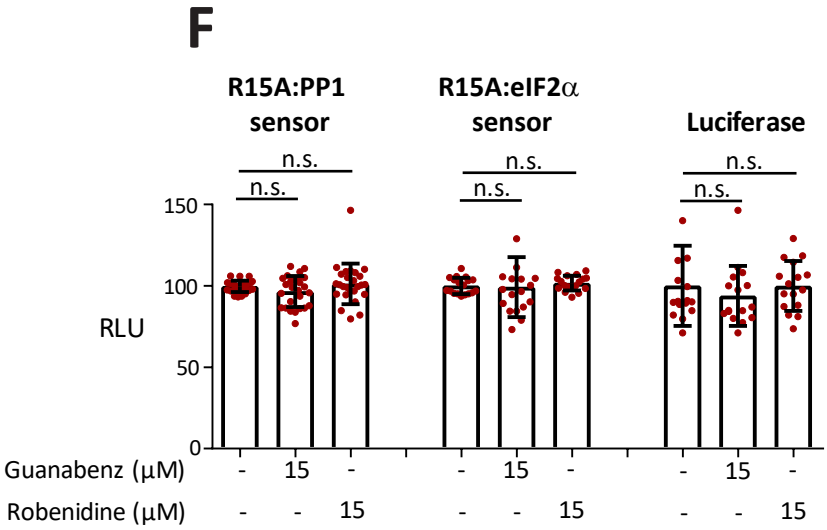
F
R15A:PP1 sensor
R15A:eIF2α sensor
Luciferase
n.s.
n.s.
n.s.
n.s.
n.s.
n.s.
RLU
150
100
50
0
Guanabenz (μM) - 15 - - 15 - - 15 -
Robenidine (μM) - - 15 - - 15 - - 15

Figure 5

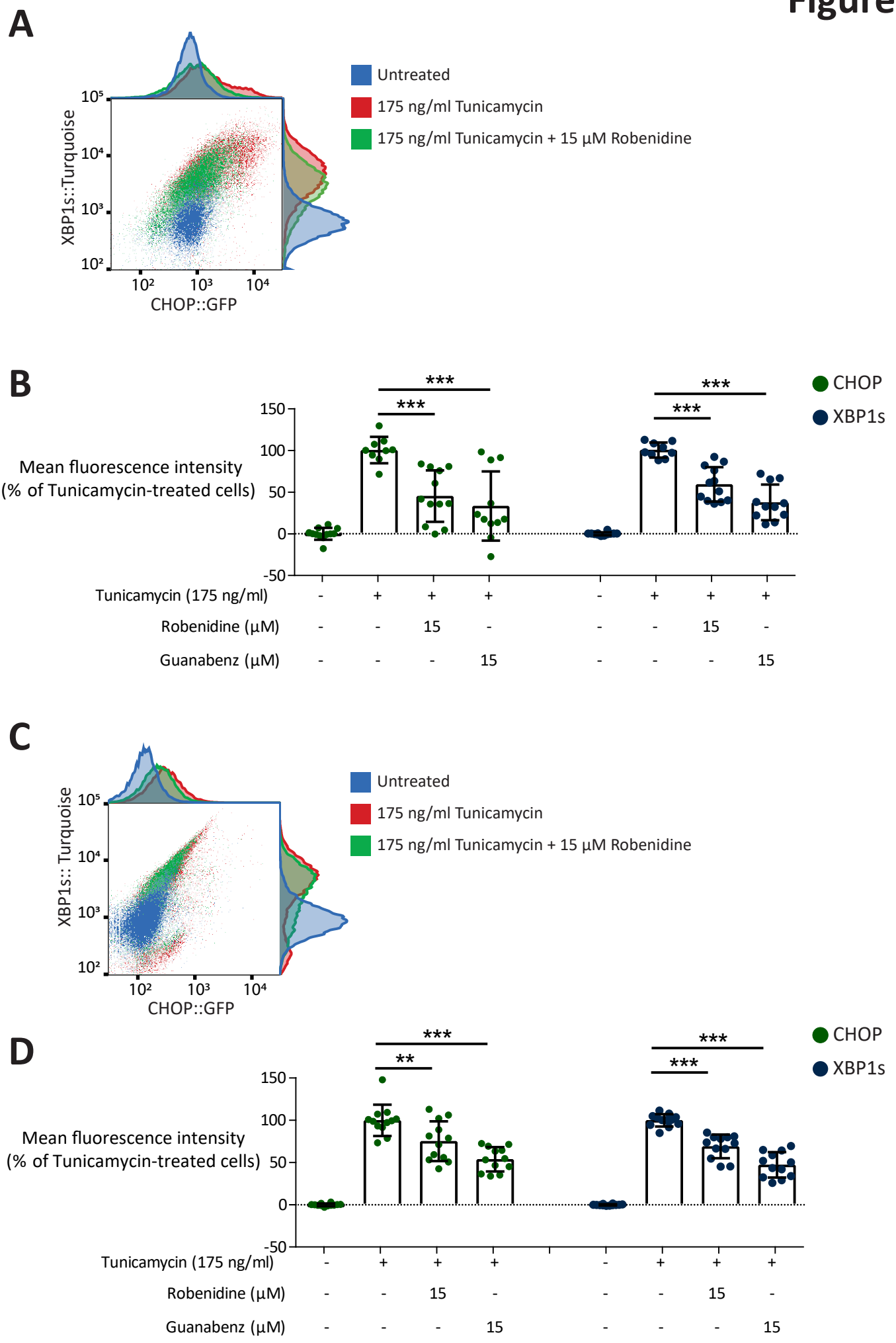
A
XBP1s::Turquoise
CHOP::GFP
Untreated
175 ng/ml Tunicamycin
175 ng/ml Tunicamycin + 15 µM Robenidine
B
Mean fluorescence intensity
(% of Tunicamycin-treated cells)
CHOP
XBP1s
Tunicamycin (175 ng/ml)
Robenidine (µM)
Guanabenz (µM)
C
XBP1s:: Turquoise
CHOP::GFP
Untreated
175 ng/ml Tunicamycin
175 ng/ml Tunicamycin + 15 µM Robenidine
D
Mean fluorescence intensity
(% of Tunicamycin-treated cells)
CHOP
XBP1s
Tunicamycin (175 ng/ml)
Robenidine (µM)
Guanabenz (µM)

The antibiotic robenidine exhibits guanabenz-like cytoprotective properties by a mechanism independent of protein phosphatase PP1:PPP1R51A

Zander Claes, Marloes Jonkhout, Ana Crespillo-Casado and Mathieu Bollen

J. Biol. Chem. published online July 23, 2019
